

## REMINERALIZATION OF TOOTH ENAMEL WITH HYDROXYAPATITE NANOPARTICLES: AN *IN VITRO* STUDY

Diana Alexandra FLOREA<sup>a</sup>, Aurora MOCANU<sup>a</sup>,  
Lucian Cristian POP<sup>a,\*</sup>, Gheorghe TOMOAI<sup>b,c</sup>,  
Cristina-Teodora DOBROTA<sup>d</sup>, Csaba VARHELYI Jr.<sup>a</sup>,  
Maria TOMOAI-COTISEL<sup>a,c,\*</sup>

**ABSTRACT.** The use of toothpastes is the best way to combat enamel loss and degradation. When they also contain hydroxyapatite nanoparticles, HAP NPs, the tooth enamel can be restored by remineralization. In this study, we developed two types of toothpastes, one with nano sized HAP, noted P1, and the other with nano multi-substituted hydroxyapatite (ms-HAP, HAP-Mg-Zn-Si), noted P2, which were used to treat the artificially demineralized teeth enamel surface. The remineralization efficacy of the two toothpastes was determined on artificially created enamel lesions by suspending healthy enamel slices in demineralizing solution, made of orthophosphoric acid of 37.5% for 90 s. For this purpose, six extracted third molars were collected and twenty-four enamel slices were cut and arbitrarily allocated to the four groups, namely n = 6 enamel slices for each group. One group served as untreated (natural) enamel control, and another group comprised demineralized enamel and two test groups, firstly demineralized, and then, they were treated with toothpastes P1 and P2, respectively, each of them for ten days, and finally were noted P1 and P2 enamel surfaces. The surface morphology and roughness of all enamel

<sup>a</sup> Babeş-Bolyai University, Research Center of Physical Chemistry, Faculty of Chemistry and Chemical Engineering, 11 Arany Janos str., RO-400028, Cluj-Napoca, Romania.

<sup>b</sup> Iuliu Hatieganu University of Medicine and Pharmacy, Department of Orthopedics and Traumatology, 47 Gen. Traian Mosoiu str., RO-400132, Cluj-Napoca, Romania.

<sup>c</sup> Academy of Romanian Scientists, 3 Ilfov str., RO-050044, Bucharest, Romania.

<sup>d</sup> Babeş-Bolyai University, Department of Molecular Biology and Biotechnology, Faculty of Biology and Geology, 44 Republicii Street, RO-400015, Cluj-Napoca, Romania.

\* Corresponding authors: Maria Tomoia-Cotisel, maria.tomoia@ubbcluj.ro; Lucian Cristian Pop, lucian.pop@ubbcluj.ro



specimens were studied by atomic force microscopy (AFM) before and after applying the treatment with the toothpastes. The toothpastes effect was evidenced by the average diameter of ceramic nanoparticles deposited within the superficial smooth layer on enamel surface having, at the completion of 10 days treatment, a low surface roughness close to that of natural enamel. This *in vitro* comparative study demonstrated that both toothpastes P1 and P2 can promote surface enamel repair by remineralization and the formation of a protective hydroxyapatite coating layer on the enamel surface treated with these toothpastes.

**Keywords:** *hydroxyapatite, multi-substituted hydroxyapatite, toothpastes, enamel remineralization, morphology, surface roughness, AFM*

## INTRODUCTION

According to the 'Global Oral Health Status Report' for 2022 published by the World Health Organisation, more than a third of the planet's population (about 2.5 billion) lives with untreated tooth decay [1].

Dental caries is a disease caused by selected oral bacteria, that demineralize and destroy the tooth enamel [2]. This highly prevalent disease appear when bacteria in the mouth determine the pH to drop reaching values that provoke erosion of the enamel surface creating in this way grooves and cavities [3]. A continual imbalance between pathological and protective factors results in dissolution of hydroxyapatite nanoparticles, HAP NPs, and consequently, in the loss of calcium, phosphate and other components from the tooth enamel, leading to enamel demineralization.

People of all ages can be affected by dental demineralization and caries, but children, older adults, people with poor oral hygiene habits and those who consume food with a high sugar content and acidic foods are particularly susceptible [4-6]. To avoid the tooth decay, an effective method is brushing with a toothpaste containing active substances [7].

More than half a century ago (around 1970), the National Aeronautics and Space Administration (NASA, U.S.) first proposed a synthetic hydroxyapatite, as a repairing material for the lost minerals of astronauts from bones and teeth due to lack of gravity [8]. Then, in 1978 the first toothpaste containing nano-HAP was prepared to repair the dental enamel. In 2006, a toothpaste comprising synthetic HAP as an alternative to fluoride occurred in Europe for the reparation of tooth enamel [8].

In recent years, to enhance the remineralization processes and reduce the demineralization, the formulation of some toothpastes with hydroxyapatite [9-12] or with hydroxyapatite doped with various elements, like Zn [13], Mg [14], and Sr [15], has been studied.

Hydroxyapatite is the core inorganic component of human bone and teeth, due to its similarity in chemical composition to the mineral components of hard tissue, and it is biocompatible. Because of its ability to bond with bone tissue through osseointegration, hydroxyapatite is widely used in bone grafts and dental implants, playing the role of a scaffold material to support the growth of new bone tissue [16, 17]. Furthermore, when HAP NPs come into contact with tooth enamel, they can bond on enamel surface replenishing the lost minerals through a process called remineralization increasing mechanical resistance and protection against dental caries [18, 19]. The HAP NPs can generate a coating layer that adheres to the tooth enamel surface, strengthening and repairing the damaged tooth enamel [20].

The following elements are also recognised to have valuable effects on dental health: magnesium [21], important for maintaining healthy teeth helping to promote the remineralization of enamel, zinc [22], essential for maintaining the structural integrity of tooth enamel helping to prevent tooth decay and cavities, strontium [23], shown to enhance the remineralization of enamel and Si [24], significant for increasing the resistance of teeth to acid erosion, and accelerating the reparation processes. Their presence in the structure of multi-substituted nano-HAP, ms-HAP, such as HAP-Mg-Zn-Sr-Si, can strengthen the enamel surface and make it more resistant to acid erosion, also promoting the deposition of new ms-HAP NPs on the enamel surface.

Owing to the size of nanoparticles, which significantly enhance the surface area, [25-28] the nano-HAP found in toothpastes has a considerable affinity for binding with proteins [29]. Additionally, nano-HAP fills in small craters and depths on the enamel surface [18]. The HAP nanoparticles of average size about 40 nm make up natural enamel. Some studies have shown the toothpaste formulations with medium or high nano-HAP content (e.g., 5% [30, 31], 10% [32-34], 15% [35], 20% [36, 37]) to promote remineralization and inhibit tooth decay. Taking into account the fact that the poorer population cannot afford to spend a lot on oral hygiene, we thought of producing a paste with a lower HAP content (about 4.0%), therefore cheaper, but which would keep its remineralizing properties.

Having all this in mind, we prepared two toothpastes, one with nano-HAP, henceforth called P1, and the other with multi-substituted nano-HAP with Mg, Zn and Si (ms-HAP, HAP-Mg-Zn-Si), henceforth called P2. The content of ceramic particles in each toothpaste is 4.0% and the average size of nano hydroxyapatites (nano-HAPs) is in range of 30 to 40 nm.

For the first time, the remineralization property of the toothpaste containing HAP-1.34 wt% Zn-2.5 wt% Mg-2.9 wt% Si was studied in comparison with the toothpaste comprising nano-HAP, on human teeth extracted for orthodontic reasons. Further, this study aims to assess the remineralization capability of these pastes, using AFM-based approaches to explore the surface morphology and roughness of surface enamel ultrastructure.

## RESULTS AND DISCUSSION

The surface morphology and roughness changes in enamel structure because of demineralization-remineralization procedures were characterized at nanoscale resolution by atomic force microscopy before and after applying the treatment with the toothpastes, P1 and P2. Therefore, the goal of this work was to optimize AFM approach in tapping mode to characterize the enamel ultrastructure, by AFM images, like 2D and 3D topographies, as well as phase and amplitude images. These AFM images are also used to determine the hydroxyapatite nanoparticle size and surface roughness at the nanoscale in environmental conditions. They are associated with the treatment of artificially demineralized enamel with toothpastes and compared with the natural enamel ultrastructure.

For this investigation, six healthy human third molars were extracted, for orthodontic reasons, and used to prepare 24 enamel slices, divided into 4 groups, each with  $n = 6$  slices; one control group of natural enamel, which did not receive toothpaste treatment. The 18 enamel slices were artificially demineralized, using orthophosphoric acid 37.5%. They were divided into 3 groups: a group ( $n = 6$ ) of demineralized samples, which were deposited into artificial saliva or physiologic serum, and 12 slices that formed two experimental groups, and each group had  $n = 6$  demineralized enamel slices; they were treated with toothpaste, namely test group P1 treated with toothpaste P1 and test group P2, treated with toothpaste P2.

AFM images are given in Figures 1 to 4 for the healthy and untreated enamel (Figure 1), for artificially demineralized enamel (Figure 2), remineralized enamel treated for 10 days, with P1 toothpaste (named P1 enamel slice, Figure 3) and treated with P2 toothpaste (called P2 enamel surface, Figure 4). AFM 2D and 3D topographic images, as well as phase and amplitude images, are displayed for scanned area of  $1 \mu\text{m} \times 1 \mu\text{m}$ .

REMINERALIZATION OF TOOTH ENAMEL WITH HYDROXYAPATITE NANOPARTICLES:  
AN *IN VITRO* STUDY

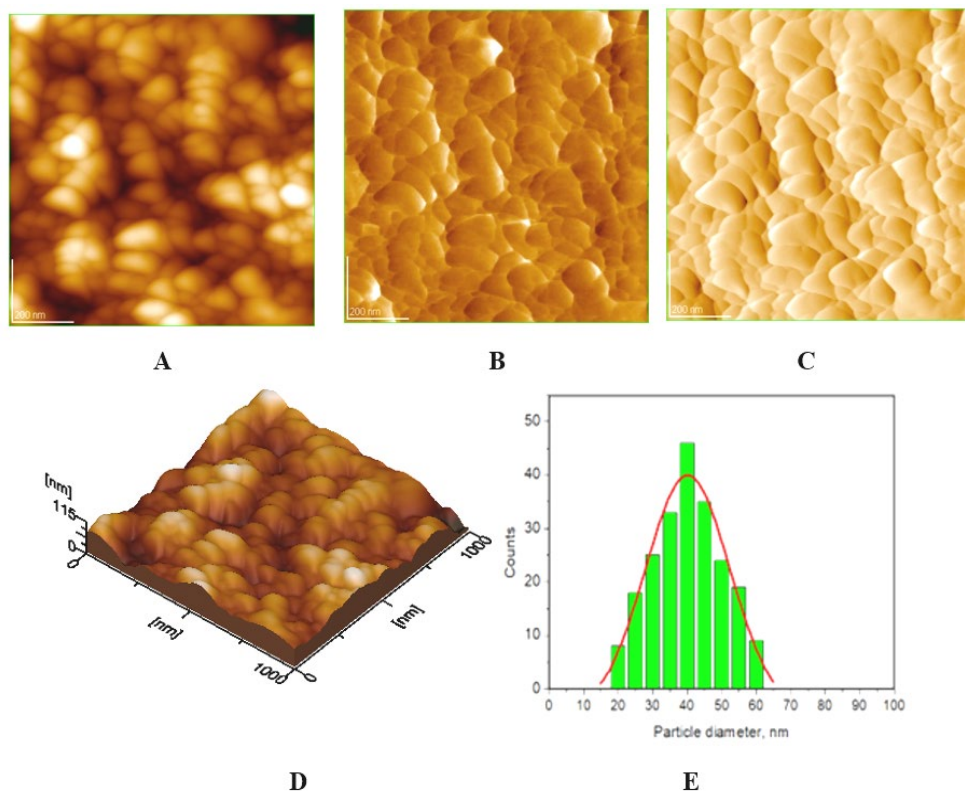


**Figure 1.** AFM images of healthy, untreated (original) enamel: 2D topography image (A), phase image (B), amplitude image (C), and 3D topography image (D), for scanned area of  $1\ \mu\text{m} \times 1\ \mu\text{m}$ , and the histogram (E) on image (A): Gaussian distribution (full line) of biological hydroxyapatite, HAP, nanoparticles diameter on tooth enamel surface (A); average diameter is  $40 \pm 3\ \text{nm}$ .

The ultrastructure of healthy, original enamel slice investigated by AFM is shown in Figure 1. From 2D topography image (A), phase (B) and amplitude (C) image, as well as from 3D height reconstruction image (D), a stable morphology is observed showing the biological HAP nanoparticles of globular shape, rather well arranged on enamel surface with an average size of 40 nm, which is proved by the particle size distribution histogram given in Figure 1E.

The demineralization process is usually used during the dental treatment, in order to expose the fresh biological HAP NPs on the enamel surface for the accurate adhesion of the restorative material to the enamel

surface. In our study, the artificially demineralized enamel is used for a potential restoration of dental enamel with synthetic hydroxyapatite nanoparticles, from toothpastes.

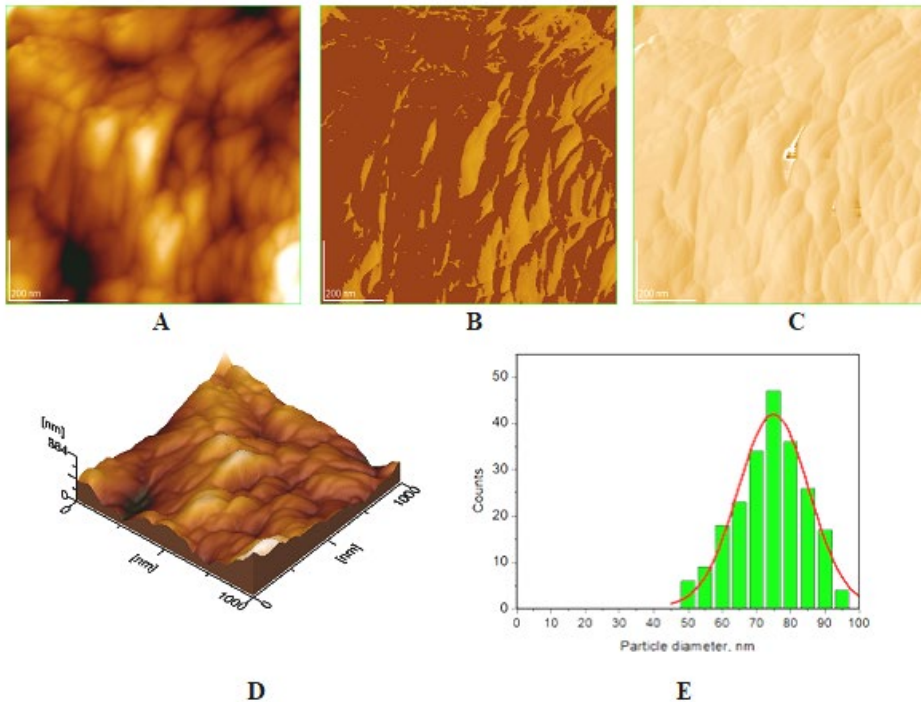


**Figure 2.** AFM images of artificially demineralized enamel: 2D topography image (A), phase image (B), amplitude image (C), and 3D topography image (D), for scanned area of  $1 \mu\text{m} \times 1 \mu\text{m}$ , and the histogram (E) on image (A): Gaussian distribution (full line) of HAP nanoparticles diameter on tooth enamel surface (A); average diameter is  $75 \pm 6 \text{ nm}$ .

The ultrastructure of demineralized enamel slice is shown in Figure 2, proving a different morphology of biological HAP nanoparticles on enamel surface.

Substantial changes in the morphology of the demineralized fresh enamel with orthophosphoric acid are observed (Figure 2A-D) with an average particle size of 75 nm (Figure 2E). Interestingly, the AFM phase image (Figure 2B) evidenced the presence of 2 phases: one dark brown (showing HAP

REMINERALIZATION OF TOOTH ENAMEL WITH HYDROXYAPATITE NANOPARTICLES:  
AN *IN VITRO* STUDY

particles), and the other one yellowish brown (proving the protein subunits), in total agreement with the fact that the HAP NPs assemblies are covered and protected with a layer of protein subunits. This situation is also shown in Figure 1B, but the presence of protein amount is reduced on the healthy enamel surface due to a natural surface erosion. The AFM 3D image (Figure 2D) confirms the globular shape of fresh biological HAP nanoparticles.

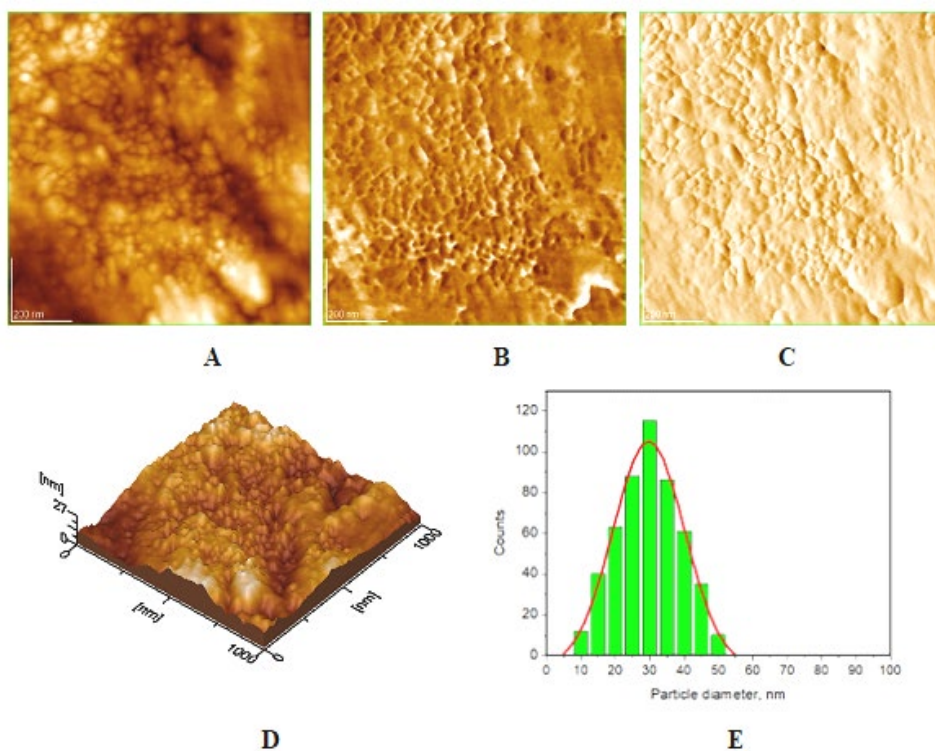


**Figure 3.** AFM images of remineralized enamel treated for 10 days with P1 toothpaste: 2D topography image (A), phase image (B), amplitude image (C), and 3D topography image (D), for scanned area of  $1 \mu\text{m} \times 1 \mu\text{m}$ , and the histogram (E) on image (A): Gaussian distribution (full line) of HAP nanoparticles diameter on remineralized tooth enamel surface (A); average diameter is  $30 \pm 4 \text{ nm}$ .

This average size of biological HAP nanoparticles (of about 75 nm) is bigger when compared with the average size of HAP nanoparticles (around 40 nm) arranged on the healthy enamel surface (Figure 1). This finding

demonstrates that the biological HAP nanoparticles on the healthy enamel surface are smaller than the ones existing inside the enamel due to the surface erosions during life time.

The AFM images of P1 remineralized enamel surface, treated for 10 days with P1 toothpaste, are presented in Figure 3A-D. These images illustrate the surface morphology of enamel surface confirming the globular aspect of HAP nanoparticles, which are homogeneous distributed on enamel surface, showing an average diameter of 30 nm as evidenced in Figure 3E. This result is in agreement with the composition of P1 toothpaste, which comprises a low crystallinity synthetic HAP, having small HAP nanoparticles of average diameter of about 30 nm, as previously was demonstrated, both in AFM and TEM images [38]. These results can be associated with the formation of a coating layer of synthetic HAP nanoparticles well spread on enamel surface, and thus, reducing the depths and various lesions on the enamel surface created due to demineralizing process.

The AFM images of P2 remineralized enamel surface, treated for 10 days with P2 toothpaste, are given in Figure 4A-D. These AFM images exposed the synthetic ms-HAP nanoparticles, as very well packed on the enamel surface (Figure 4B, C), having ms-HAP nanoparticles with mean diameter of about 40 nm (Figure 4E) on the remineralized tooth enamel surface (Figure 4A).

It is meaningful to remark that the P2 toothpaste comprises a low crystallinity multi-substituted HAP nanoparticles, HAP-Mg-Zn-Si, of average diameter of about 40 nm, as previously was demonstrated, both in AFM and SEM images, coupled with XRD and SEM-EDX, showing its chemical composition and crystallinity [39].

The topographic features of the ms-HAP nanoparticles deposited on P2 enamel surface are presented in Figure 4A, D. These particles are spherical smoothed ms-HAP particles with mean diameter of about 40 nm, coinciding as size with that of biological HAP on natural, enamel. This resemblance might increase the repair potential of toothpaste P2 leading to an enhanced remineralization of tooth enamel in comparison with toothpaste P1.

In order to explore the structural differences [40] among enamel samples by using AFM, the surface roughness values: arithmetical roughness,  $R_a$ , and root mean square roughness,  $R_{RMS} = R_q$ , with their standard deviations (calculated from minimum three different investigated scanned areas) for untreated, demineralized and remineralized enamel surfaces with the two toothpastes, P1 and P2, are presented in Figure 5.

REMINERALIZATION OF TOOTH ENAMEL WITH HYDROXYAPATITE NANOPARTICLES:  
AN *IN VITRO* STUDY

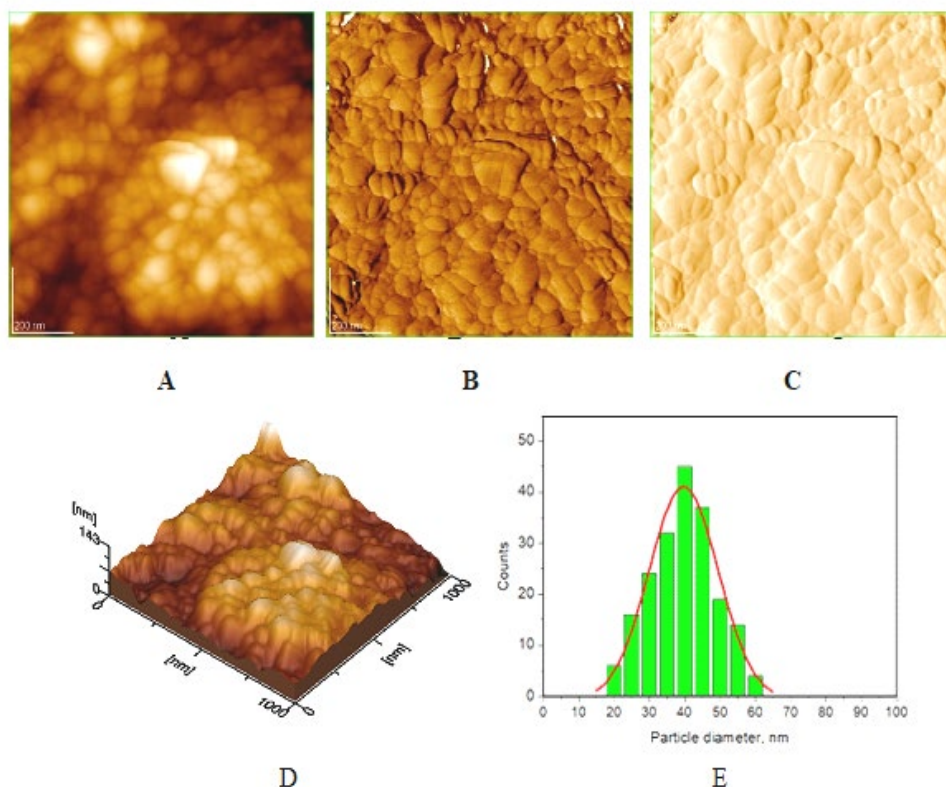


**Figure 4.** AFM images of remineralized enamel treated for 10 days with P2 toothpaste: 2D topography image (A), phase image (B), amplitude image (C), and 3D topography image (D), for scanned area of 1  $\mu\text{m}$  x 1  $\mu\text{m}$ , and the histogram (E) on image (A): Gaussian distribution (full line) of HAP nanoparticles diameter on remineralized tooth enamel surface (A); average diameter is  $40 \pm 2$  nm.

Examining the surface nano-roughness (Figures 5A and 5B) it can be appreciated that the values for Ra and Rq have the same pattern. Enamel samples 3 and 4 have both roughness values closer (in the error range) to original enamel sample 1 demonstrating an efficient restoration of surface enamel by the coating with a protective synthetic hydroxyapatite layer, deposited on the enamel surface, treated with the toothpastes P1 and P2, while sample 2 have an increased roughness due to the demineralization process.

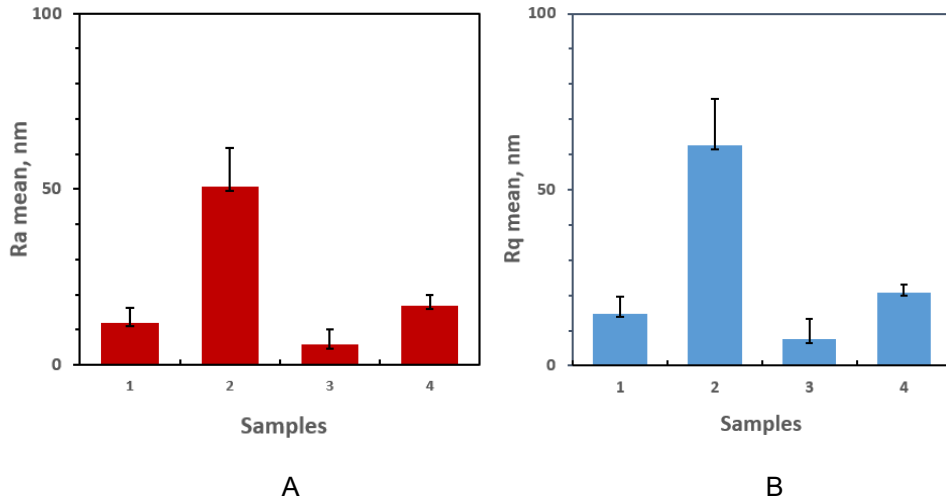


**Figure 5.** Surface roughness on enamel samples, (A) Ra and (B) Rq ( $R_{RMS}$ ), for: natural enamel (1), artificially demineralized enamel (2), and demineralized enamel surface treated with toothpaste P1 (3), and treated with toothpaste P2 (4), at 10 days of enamel treatment.

The uniformity of the HAP nanoparticles on the natural enamel surface gives low values of surface roughness values:  $R_{RMS}$  of about 14 nm and Ra approximately 12 nm. The roughness of the enamel nanostructure was significantly changed after phosphoric acid erosion (sample 2), with an Ra of about 50 nm and  $R_{RMS}$  of 62 nm. Similar results are comparable to the ones reported in literature for enamel roughness after phosphoric acid etching [41].

This study disclosed that the toothpastes P1 and P2 are rather similar in their action on enamel surface, promoting the remineralization of enamel surface in 10 days. However, toothpaste P2 generated a stable morphological coating layer on enamel surface as judged by AFM. These results revealed that the toothpaste P2 might be more active than toothpaste P1, taking into account the contribution of substituting elements: Mg, Zn and Si on bone and enamel repair and restoration [41, 42]. These toothpastes might be used in dental oral care to protect and mineralized the enamel surface.

Clearly, AFM approach is a great technique for exploring the surface morphology and surface roughness of dental enamel and thus, is suitable for assessing the real efficacy of toothpastes in the ongoing remineralizing and restoring action on the dental surface.

## CONCLUSIONS

Both toothpastes containing stoichiometric synthetic hydroxyapatite, P1, and multi-substituted hydroxyapatite, P2, were developed and used to treat artificially demineralized enamel surface. The remineralization efficacy of these toothpastes was determined on artificially demineralized enamel. The P2 toothpaste proved to be the best of the two, leading to stable morphological modifications of the dental enamel surface. In the ten treatment days, the demineralized enamel lesions were remineralized completely as shown by AFM investigations, of structural-morphology and surface roughness. Judging from the AFM results, these toothpastes can be used as potential agents for remineralization of enamel surface.

This *in vitro* comparative study demonstrates that both toothpastes P1 and P2 may promote surface enamel repair by the formation of a protective hydroxyapatite (HAP or ms-HAP) coating on the demineralized enamel surface. These synthetic ceramic nanoparticles formed a regularly arrangement within the superficial smooth coating layer on the enamel surface, after the course of treatment, assuring a low surface roughness close to that of the natural enamel, providing further evidence of the toothpaste's efficacy.

## FUTURE DIRECTIONS

The biomimetic approach to enamel remineralization will be extended in our Scientific Research Center of Physical Chemistry at Babes-Bolyai University of Cluj-Napoca, under the leadership of Professor Maria Tomoaia-Cotisel, the Director of this Center. Therefore, through the use of plant extracts, with anti-inflammatory and anti-microbial effect, in biomimetic toothpastes, an enhanced remineralization of enamel subsurface lesions might be achieved with a better protection of the enamel against dental caries. For this purpose, the atomic force microscopy, AFM, from this Research Center will be further used in operating tapping and contact modes. Consequently, a major aim of contemporary dentistry will be fulfilled regarding the management of non-cavitated caries, by involving innovative biomimetic remineralization systems to restore the teeth strength and esthetic appearance increasing the dental resistance to future acid challenge.

## EXPERIMENTAL SECTION

### ***Materials***

The stoichiometric hydroxyapatite, HAP, and multi-substituted hydroxyapatite, HAP-1.34wt%Zn-2.5 wt% Mg-2.9 wt% Si, of low crystallinity have been synthesized employing a wet chemical precipitation process at low temperature, as described elsewhere [39], [42-44]. Orthophosphoric acid (85 wt. % in H<sub>2</sub>O) was purchased from Sigma-Aldrich.

### ***Toothpastes preparation***

For the preparation of the toothpastes the following Sigma-Aldrich chemicals were purchased and used as such, without further purification: sorbitol (≥98%), glycerin (≥99.0%), sodium dodecyl sulfate, (≥99.0%), silicon dioxide (nanopowder, 10-20 nm particle size, 99.5% trace metals basis), and xanthan gum from *Xanthomonas campestris* (yellow powder).

Toothpastes were prepared by mixing the following ingredients in the proportions shown in brackets (weight percent, wt%): distilled water (64.4), glycerin (24.2), sorbitol (3.1), silicon dioxide (3.7), hydroxyapatite (4.0), xanthan gum (0.3), sodium dodecyl sulphate (0.3). In the case of toothpaste P1, stoichiometric hydroxyapatite was used, and in the case of toothpaste P2, the multi-substituted hydroxyapatite (HAP-1.34 wt% Zn - 2.5 wt% Mg-2.9 wt% Si) was used. The prepared toothpastes were used to remineralize the artificially demineralized dental enamel.

### ***Protocol for obtaining enamel slices***

This study used 6 healthy human third molars that had been extracted for orthodontic reasons.

A total of 24 slices of 1.5 mm thick enamel longitudinal samples were collected and distributed into 2 sets; one control group, with n = 6 slices, of natural enamel, which did not receive toothpaste treatment and a group of 18 enamel slices, which were artificially demineralized, for 90 seconds, using orthophosphoric acid 37.5%. They were divided into 3 groups: a group (n = 6) demineralized enamel samples, which were deposited into artificial saliva (Mission Pharmacal Company, San Antonio, USA) and 12 slices that formed two experimental groups, and each group had n = 6 demineralized enamel slices; they were treated with toothpaste, namely test group P1 treated with toothpaste P1 and test group P2, treated with toothpaste P2.

Brushing the demineralized teeth (from test groups) for 3 minutes twice a day with each toothpaste is performed each day, for 10 days, to selected artificially demineralized enamel surfaces. All enamel samples were examined in the AFM laboratory from Scientific Research Center in Physical Chemistry, at Babes-Bolyai University of Cluj-Napoca.

**AFM approach** was carried out employing a JSPM 4210 Scanning Probe Microscope, Jeol, Japan. We assessed the surface morphology and roughness in accordance with our prior work [45-52]. The AFM images were obtained on scanned area of 1  $\mu\text{m}$  x 1  $\mu\text{m}$  in tapping mode, employing NSC 15 Hard cantilevers manufactured by Micromesh Co, Estonia and processed in the standard manner using the specific soft Win SPM2.0 Processing, Jeol, Japan. The resonance frequency of the cantilever is about 325 kHz and the force constant is around of 40 N/m.

### **Statistical data**

Nano-roughness  $R_a$  and  $R_{RMS} = R_q$  were determined by using AFM 3D images and calculated with the specific AFM soft from at least three independent scanned areas for each enamel specimen and expressed as mean  $\pm$  standard deviation. The mean diameter of nanoparticles of hydroxyapatites on enamel surface was determined from at least three independent calculated histograms, each obtained on three different scanned areas of 1  $\mu\text{m}$  x 1  $\mu\text{m}$ , and on each enamel specimen.

### **ACKNOWLEDGMENTS**

This work was supported by grants from the Ministry of Research, Innovation and Digitization, CNCS/CCCDI-UEFISCDI, project number 186 within PNCDI III.

### **REFERENCES**

1. Global oral health status report: towards universal health coverage for oral health by 2030. Geneva: World Health Organization; **2022**, ISBN 978-92-4-006148-4.
2. J.D.B. Featherstone; *J. Dent. Res.*, **2004**, 83, 1, 39-42.
3. A. Belmok; J.A. de Cena; C.M. Kyaw; N. Damé-Teixeira; *J. Dent. Res.*, **2020**, 99, 6, 630-643.
4. D.J. Bradshaw; R.J.M. Lynch; *Int. Dent. J.*, **2013**, 63, 64-72.
5. A.C.R. Tanner; C.A. Kressirer; S. Rothmiller; I. Johansson; N.I. Chalmers; *Adv. Dent. Res.*, **2018**, 29, 1, 78-85.

6. A. Shimada; M. Noda; Y. Matoba; T. Kumagai; K. Kozai; M. Sugiyama; *Biosci. Microbiota Food Health*, **2015**, *34*, 2, 29-36.
7. T. Lubna; N. Rabia; Etiology and Remedy through Natural Resources, in *Dental Caries-Diagnosis, Prevention and Management*, A., Zühre, Ed.; IntechOpen, London, UK, **2018**, Chapter 3, pp 19-33.
8. E. Pepla; L.K. Besharat; G. Palaia; G. Tenore; G. Migliau; *Ann Stomatol*, **2014**, *5*, 3, 108-114.
9. T.Sato; M. Niwa; W. Li; H. Aoki; H. Aoki; T. Daisaku; *JJ Mater Sci Mater Med*, **2001**, *12*, 277-281.
10. K. O'Hagan-Wong; J. Enax; F. Meyer; B. Ganss; *Odontology*, **2022**, *110*, 2, 223-230.
11. H. Limeback; J. Enax; F. Meyer; *Biomimetics (Basel, Switzerland)*, **2023**, *8*, 1, 23.
12. A.M.C Leal; M.V.B. dos Santos; E.C. da Silva Filho; A.L. Menezes de Carvalho; C.P.M. Tabchoury; G.C.Vale; *Int. J. Nanomedicine*, **2020**, *15*, 7469-7479.
13. C. Poggio; C. Gulino; M. Mirando; M. Colombo; G. Pietrocola; *J. Clin. Exp. Dent.*, **2017**, *9*, 1, e118-e122.
14. M. Polyakova; I. Sokhova; V. Doroshina; M. Arakelyan; N. Novozhilova; K. Babina; *J. Int. Soc. Prev. Community Dent.*, **2022**, *12*, 2, 252-259.
15. M.G. Cagetti; F. Cocco; R.J. Wierichs; T.G. Wolf; C. Salerno; A. Arghittu; G. Campus; *J. Dent.*, **2022**, *121*, 104049.
16. V.S. Kattimani; S. Kondaka; K.P. Lingamaneni; *Bone tissue regen. insights*, **2016**, *7*, BTRI.S36138.
17. I. Ielo; G. Calabrese; G. De Luca; S. Conoci; *Int. J. Mol. Sci.*, **2022**, *23*, 17, 9721.
18. A.C. Ionescu; G. Cazzaniga; M. Ottobelli; F. Garcia-Godoy; E. Brambilla; *J. Funct. Biomater.*, **2020**, *11*(2), 36.
19. K. O'Hagan-Wong; J. Enax; F. Meyer; B. Ganss; *Odontology*, **2022**, *110*, 2, 223-230.
20. R. Sebastian; S.T. Paul; U. Azher; D. Reddy; *Int. J. Clin. Pediatr. Dent.*, **2022**, *15*, 1, 69-73.
21. E. Klimuszko; K. Orywal; T. Sierpinska; J. Sidun; M. Golebiewska; *Odontology*, **2018**, *106*, 4, 369-376.
22. R.J.M. Lynch; *Int. Dent. J.*, **2011**, *61*, 46-54.
23. L.L. Dai; F. Nudelman; C.H. Chu; E.C.M. Lo; M.L. Mei; *J. Dent.*, **2021**, *105*, 103581.
24. T.G. Khonina; O.N. Chupakhin; V.Ya. Shur; A.P. Turygin; V.V. Sadovsky; Yu.V. Mandra; E.A. Sementsova; A.Yu. Kotikova; A.V. Legkikh; E.Yu. Nikitina; E.A. Bogdanova; N.A. Sabirzyanov; *Colloids Surf. B*, 189, **2020**, 110851
25. A.A. Balhaddad; A.A. Kansara; D. Hidan; M.D. Weir; H.H.K. Xu; M.A.S. Melo; *Bioact. Mater.*, **2019**, *4*, 43-55.
26. N. Juntavee; A. Juntavee; P. Plongniras; *Int J Nanomedicine*, **2018**, *13*, 2755-2765.
27. F. Carrouel; S. Viennot; L. Ottolenghi; C. Gaillard; D. Bourgeois; *Nanomater.*, **2020**, *10*, 140.
28. M.A. Melo; S.F. Guedes; H.H. Xu; L.K. Rodrigues; *Trends Biotechnol*, **2013**, *31*, 8, 459-467.
29. L. Chen; S. Al-Bayatee; Z. Khurshid; A. Shavandi; P. Brunton; J. Ratnayake, *Materials (Basel)*, **2021**, *14*, 17.
30. T. Rodemer; N. Pütz; M. Hannig; *Sci. Rep.*, **2022**, *12*, 1, 17612.

31. K. Najibfard; K. Ramalingam; I. Chedjieu; B.T. Amaechi; *J. Clin. Dent.*, **2011**, *22*, 5, 139-143.
32. B.T. Amaechi; P.A. Azees; D.O. Alshareif; M.A. Shehata; P.P.d.C.S. Lima; A. Abdollahi; P.S. Kalkhorani; V. Evans; *BDJ Open*, **2019**, *5*, 1, 18.
33. B.M. Souza; L.P. Comar; M. Vertuan; C. Fernandes Neto; M.A.R. Buzalaf; A.C. Magalhães; *Caries Res.*, **2015**, *49*, 5, 499-507.
34. S.B. Huang; S.S. Gao; H.Y. Yu; *Biomed Mater*, **2009**, *4*, 3, 034104.
35. B.T. Amaechi; P.A. Azees; L.O. Okoye; F. Meyer; J. Enax; *BDJ Open*, **2020**, *6*, 1, 9.
36. B.T. Amaechi; R. Farah; J.A. Liu; T.S. Phillips; B.I. Perozo; Y. Kataoka; F. Meyer; J. Enax, *BDJ Open*, **2022**, *8*, 1, 33.
37. P. Tschoppe; D.L. Zandim; P. Martus; A.M. Kielbassa; *J. Dent.*, **2011**, *39*, 6, 430-437.
38. R. Balint; A. Mocanu; C. Garbo; L. Timis; I. Petean; O. Horovitz; M. Tomoaia-Cotisel, *Stud. UBB Chem*, **2017**, *62*, 2, 95-103.
39. J.L. C. Garbo; M. D'Este; G. Demazeau; A. Mocanu; C. Roman; O. Horovitz; M. Tomoaia-Cotisel, *Int J Nanomedicine*, **2020**, *15*, 1037- 1058.
40. L.Z. Racz; G.-A. Paltinean; I. Petean; Gh. Tomoaia; L.C. Pop; G. Arghir; E. Levei; A. Mocanu; C.-P. Racz; M. Tomoaia-Cotisel; *Stud. UBB Chem*, **2022**, *67*, 3, 61-74.
41. J.P. Loyola-Rodriguez; V. Zavala-Alonso; E. Reyes-Vela; N. Patiño-Marin; F. Ruiz; K.J. Anusavice; *J. electron microsc.*, **2010**, *59*, 2, 119-125.
42. C. Garbo; M. Sindilaru; A. Carlea; G. Tomoaia; V. Almasan; I. Petean; A. Mocanu; O. Horovitz; M. Tomoaia-Cotisel; *Part. Sci. Technol.*, **2017**, *35*, 1, 29-37.
43. D. Oltean-Dan; G.B. Dogaru; M. Tomoaia-Cotisel; D. Apostu; A. Mester; H.R. Benea; M.G. Paiusan; E.M. Jianu; A. Mocanu; R. Balint; C.O. Popa; C. Berce; G.I. Bodizs; A.M. Toader; G. Tomoaia; *Int J Nanomedicine*, **2019**, *14*, 5799-5816.
44. A. Mocanu; O. Cadar; P.T. Frangopol; I. Petean; G. Tomoaia; G.-A. Paltinean; C.P. Racz; O. Horovitz; M. Tomoaia-Cotisel; *R. Soc. Open Sci.*, **2021**, *8*, 1, 201785.
45. C.-P. Racz; L.Z. Racz; C.G. Floare; G. Tomoaia; O. Horovitz; S. Riga; I. Kacso; G. Borodi; M. Sarkozi; A. Mocanu; C. Roman; M. Tomoaia-Cotise; *Food Hydrocoll.*, **2023**, *139*, 108547.
46. D. Oltean-Dan; G.B. Dogaru; E.M. Jianu; S. Riga; M. Tomoaia-Cotisel; A. Mocanu; L. Barbu-Tudoran; G. Tomoaia; *Micromachines*, **2021**, *12*, 11, 1325.
47. G. Furtos; M.A. Naghiu; H. Declercq; M. Gorea; C. Prejmorean; O. Pana; M. Tomoaia-Cotisel; *J. Biomed. Mater. Res. Part B Appl. Biomater.*, **2016**, *104*, 7, 1290-1301.
48. U. V. Zdrenghia; G. Tomoaia; D.-V. Pop-Toader; A. Mocanu; O. Horovitz; M. Tomoaia-Cotisel; *Comb. Chem. High Throughput Screen.*, **2011**, *14*, 4, 237-247.
49. M. Tomoaia-Cotisel; A. Tomoaia-Cotisel; T. Yupsanis; Gh. Tomoaia; I. Balea; A. Mocanu; C. Racz; *Rev. Roum. Chim*, **2006**, *51*, 12, 1181-1185.
50. O. Horovitz; G. Tomoaia; A. Mocanu; T. Yupsanis; M. Tomoaia-Cotisel; *Gold Bull.*, **2007**, *40*, 4, 295-304.
51. G. Tomoaia; M. Tomoaia-Cotisel; A. Mocanu; O. Horovitz; L.D. Bobos; M. Crisan; I. Petean; *J. Optoelectron. Adv. Mater.*, **2008**, *10*, 961-964.
52. O. Monfort; L.-C. Pop; S. Sfaelou; T. Plecenik; T. Roch; V. Dracopoulos; E. Stathatos; G. Plesch; P. Lianos; *Chem. Eng. J.*, **2016**, *286*, 91-97.

